

Submitted to the Astrophysical Journal Letters

Detection of low Eu abundances in extremely metal-poor stars and the origin of *r*-process elements ¹

Yuhri Ishimaru

Department of Physics, and Graduate School of Humanities and Sciences, Ochanomizu University, 2-1-1 Otsuka, Bunkyo, Tokyo 112-8610, Japan; ishimaru@phys.ocha.ac.jp

Shinya Wanajo

Department of Physics, Sophia University, 7-1 Kioi-cho, Chiyoda-ku, Tokyo, 102-8554, Japan; wanajo@sophia.ac.jp

Wako Aoki

National Astronomical Observatory, Mitaka, Tokyo, 181-8588 Japan; aoki.wako@nao.ac.jp

and

Sean G. Ryan

Department of Physics and Astronomy, The Open University, Walton Hall, Milton Keynes, MK7 6AA, United Kingdom; S.G.Ryan@open.ac.uk

ABSTRACT

We report detailed abundance analyses for three extremely metal-poor stars with $[\text{Fe}/\text{H}] \lesssim -3$ in the Galactic halo, using the *Subaru* High Dispersion Spectrograph (HDS). All these stars are found to have sub-solar relative abundances of $[\text{Eu}/\text{Fe}]$, and exhibit the lowest $[\text{Eu}/\text{H}]$ values at their metallicities. Comparison of these low Eu abundances with our chemical evolution model of the Galactic halo implies the dominant source of Eu to be the low-mass end of the Type II supernova mass range. This suggests that collapsing O-Ne-Mg cores resulting from $8 - 10M_{\odot}$ stars are the major *r*-process site.

Subject headings: nuclear reactions, nucleosynthesis, abundances — stars: abundances — stars: Population II — supernovae: general — Galaxy: evolution — Galaxy: halo

¹Based on data collected at Subaru Telescope, which is operated by the National Astronomical Observatory of Japan.

1. Introduction

The astrophysical origin of the rapid neutron capture (*r*-process) elements is still uncertain. Although a few scenarios such as neutrino winds (Woosley et al. 1994) in type II supernovae (SNe II), the collapse of O-Ne-Mg cores resulting from $8 - 10M_{\odot}$ stars (Wanajo et al. 2003), and neutron star mergers (Freiburghaus et al. 1999) show some promise, no consensus has been achieved.

Extremely metal-poor stars in the Galactic halo are expected to provide important clues for the origin of *r*-process elements. Abundance analysis studies in the past decade have shown the existence of large scatters in measured chemical compositions of, in particular, neutron-capture elements such as Sr and Ba, and possibly Eu among metal-poor stars in the Galactic halo (e.g., McWilliam et al. 1995; Ryan, Norris, & Beers 1996). If the measured scatter accurately portrays the state of the interstellar medium (ISM) from which the stars formed, such large dispersions in excess of observational errors indicate that the ISM was not fully mixed at the early epoch of the Galactic history and that metal-poor stars contain products from only one or a few SNe II (Gilroy et al. 1988; Ryan, Norris, & Bessell 1991; Audouze & Silk 1995). The scale of scatter in relative abundance ratios possibly reflects variation in the nucleosynthetic yields of SNe from different mass progenitors, and thus, the huge dispersions in neutron-capture elements imply that the production of *r*-process elements is highly dependent on the masses of SN progenitors.

Eu is a tracer of the *r*-process. Ishimaru & Wanajo (1999, hereafter IW99) have shown by their chemical evolution model that the large star-to-star dispersion of Eu relative to Fe observed in very metal-poor stars is naturally explained if the *r*-process elements originate from a limited mass range of progenitor stars, such as the SNe II from stars of $8 - 10M_{\odot}$ or alternatively $> 30M_{\odot}$ (see also Travaglio et al. 1999). Tsujimoto, Shigeyama, & Yoshii (2000) have concluded by a similar approach that the SNe from $\approx 20M_{\odot}$ are the dominant source of the *r*-process elements. A clear difference among these cases is expected to appear in stellar distribution of $[\text{Eu}/\text{Fe}]^2$ at $[\text{Fe}/\text{H}] \lesssim -3$ (IW99; Fields, Truran, & Cowan 2002). However, a shortage of observational data in this metallicity range has made it difficult to distinguish between the *r*-process sites proposed above.

In this *Letter*, we report on the study of three extremely metal-poor stars which we show to have very low Eu abundances, using spectra obtained with the *Subaru* High Dispersion Spectrograph (HDS) (§2). Comparison of these data with our chemical evolution models enables us to distinguish between the proposed *r*-process sites (§3). Implications for the

² $[X_i/X_j] \equiv \log(N_i/N_j) - \log(N_i/N_j)_{\odot}$, where N_i indicates abundance of *i*-th element X_i .

origin of *r*-process elements are then discussed in §4.

2. Observations and Analysis

We selected three very metal-poor ($[\text{Fe}/\text{H}] \lesssim -3$) giants, HD 4306, CS 22878–101, and CS 22950–046. Previous abundance studies (e.g., McWilliam et al. 1995; Carretta et al. 2002) have found relatively low Ba abundances ($[\text{Ba}/\text{Fe}] \lesssim -1$), which nevertheless are typical of low-metallicity stars (Norris, Ryan, & Beers 2001). Observations were made with the High Dispersion Spectrograph (HDS; Noguchi et al. 2002) of the 8.2m Subaru Telescope in 2001 July. The spectra were taken with a resolving power of $R = 50,000$. The total exposure time was 50, 240, and 360 minutes for HD 4306, CS 22878–101, and CS 22950–046, respectively. Data reduction was performed in the standard way within the IRAF³ environment. The S/N ratios per 0.012 Å pixel at 4100 Å of the final spectra are 260, 110, and 80 for HD 4306, CS 22878–101, and CS 22950–046, respectively.

Equivalent widths were measured by fitting Gaussian profiles to the absorption lines of species listed in Table 1⁴, except for Eu. We focus here on neutron-capture elements, but Mg, Ca, and Ti lines were also analyzed as a check of our analysis and for future discussions. A standard LTE analysis using model atmospheres of Kurucz (1993), based on equivalent widths measured above, was performed for species other than Eu. Results are given in Table 1. In the analysis of Ba lines, we included the hyperfine splitting and isotope shifts (McWilliam 1998), assuming isotope ratios of the *r*-process component in solar system material (Arlandini et al. 1999).

The atmospheric parameters (effective temperature: T_{eff} (K), surface gravity: g (cm s^{−2}), micro-turbulent velocity: v_{mic} (km s^{−1}), and metallicity that is assumed to be $[\text{Fe}/\text{H}]$) of CS 22878–101 and CS 22950–046 were adopted from Cohen et al. (2002) and Carretta et al. (2002), i.e., $T_{\text{eff}}/\log g/[\text{Fe}/\text{H}]/v_{\text{mic}} = 4775/1.3/-3.1/2.0$, and $4730/1.3/-3.3/2.0$, respectively. We found that these gravities satisfy the ionization balance between Fe I and Fe II in both objects, and the microturbulence velocities lead to no dependence of the derived abundance on equivalent widths of Fe I lines. The derived Fe abundances also agree very well with the assumed metallicities. For this reason, we adopted their atmospheric parameters with no modification. For HD 4306, we adopted $T_{\text{eff}} = 5000$ K based on $V - K = 2.15$ (Nor-

³IRAF is distributed by the National Optical Astronomy Observatories, which is operated by the Association of Universities for Research in Astronomy, Inc. under cooperative agreement with the National Science Foundation.

⁴The line list and measurements are available on the website <http://optik2.mtk.nao.ac.jp/~waoki/EW/>

ris, Bessell, & Pickles 1988; and 2MASS data: Skrutskie et al. 1997) and the temperature scale of Houdashelt, Bell & Sweigart (2000). We derived g and v_{mic} from the analysis of our spectrum assuming the ionization balance and no dependence of the derived abundance on line strengths. The resulting parameters, $T_{\text{eff}}/\log g/[\text{Fe}/\text{H}]/v_{\text{mic}} = 5000/2.0/-3.0/1.85$, are quite similar to those of other works (McWilliam et al. 1995, Honda et al., in preparation).

A spectrum synthesis technique was applied for the three Eu II lines at 3819, 4129, and 4205 Å to measure Eu abundances. The Eu line list was produced using the data including the hyperfine splitting and isotope shifts provided by Lawler et al. (2001). Contamination by other species was included using the comprehensive line list of Kurucz (1995). Figure 1 shows comparisons between observed spectra and synthetic ones for the 3819 Å line, which is the strongest among the three lines. The Eu II line is clearly detected in the spectra of HD 4306 and CS 22878–101. On the other hand, the Eu II line is not detected in CS 22950–046, for which we determined an upper limit for the Eu abundance. We tried a similar analysis for the other two Eu lines, and found that consistent results were derived from the analysis for the 4129 Å line, while the measurement for the 4205 Å is rather uncertain because of a severe contamination by the V II line at 4205.09 Å. We adopted the average of the Eu abundances derived from the 3819 and 4129 Å lines. In Table 2, we give the equivalent widths of the Eu II lines estimated from a spectrum synthesis for the Eu abundances derived from individual lines. Since the Eu lines are not detected in the spectrum of CS 22950–046, we estimated the upper limit of equivalent widths from the 3σ depth of the noise level and typical line widths for this object, and determined an upper limit of the Eu abundance which is given in Table 1.

The random errors in the analysis are estimated from the standard deviation of the abundances derived from individual lines for each species. The values are sometimes unrealistically small when the number of lines is small. For this reason, for the random errors we adopted the larger of the value for the species and that for Fe I. These errors are 0.08–0.15 dex, depending on the species and the quality of the spectra. We estimated the errors in the Eu abundances from the fitting of synthetic spectra to the observed ones by eye, adopting 0.1 dex for HD 4306 and 0.2 dex for CS 22878–101. The errors in the abundance determinations from the uncertainties of the atmospheric parameters were evaluated for $\Delta T_{\text{eff}} = 100$ K, $\Delta \log g = 0.3$, $\Delta v_{\text{mic}} = 0.3$ km s^{−1}, and $\Delta [\text{M}/\text{H}] = 0.3$ dex for HD 4306. We derived the total uncertainty by adding in quadrature these errors and the random error estimated above, and give them in Table 1. We note that relatively large errors in [Sr/Fe] originate from the sensitivity to microturbulent velocities, because only two strong resonance lines were used in the analysis. The [Eu/Fe] values are affected most significantly (by 0.12 dex) by the uncertainty in the surface gravity (by $\Delta g = 0.3$).

Comparisons between our results for the two CS objects and those by Carretta et al. (2002) show good agreement (within 0.17 dex) for species shown in Table 1 other than Eu. An exception is the Ba abundance of CS 22878–101: our Ba abundance is 0.35 dex higher than that by Carretta et al. (2002). The equivalent widths of the Ba II 4554 Å line agree well between the two studies, and the atmospheric parameters are the same. Hence, we suspect that this discrepancy is at least partially due to the assumed isotope ratios of Ba assumed in the analysis, which affects the hyperfine structure, but which were not explicitly reported by Carretta et al. (2002).

3. Comparison with the Galactic chemical evolution models

It has been commonly stated that the scatter of relative abundance ratios among metal-poor stars is a consequence of the inhomogeneity of the ISM at the early epoch of our Galaxy. Assuming that star formation is induced by a single supernova explosion, IW99 have constructed an inhomogeneous chemical evolution model of the Galactic halo (see IW99 for details). The chemical composition of the newly formed star is taken to be a mixture of the products from each SN and the ISM swept up by the expanding ejecta, which leads to a large star-to-star scatter of relative abundances among extremely metal-poor stars. We use this chemical evolution model with some improvements (see Ishimaru, Prantzos, & Wanajo 2003) to derive the Galactic evolution of Eu, which is a tracer of the *r*-process elements. We consider three cases, where the *r*-process elements originate from stars of (a) $8 - 10M_{\odot}$, (b) $20 - 25M_{\odot}$, and (c) $> 30M_{\odot}$ stars. The interpretation of the astrophysical sites for these cases is discussed in §4.

Stellar yields for Type II and Type Ia SNe are taken from Nomoto et al. (1997a, b). The $8 - 10M_{\odot}$ stars are assumed to produce no iron, since their contribution to the enrichment of iron-peak elements in the Galaxy is negligible (Wanajo et al. 2003). The mass of Eu produced is assumed to be constant over the mass range of each case, which is determined to match the solar value of [Eu/Fe] at [Fe/H] = 0. Figure 2 compares the results of these cases with the observational data presented in §2 (large circles), together with the data from other sources cited in the caption (small circles). We exclude two peculiar stars; an *s*-process rich star, CS 22898–027 (McWilliam et al. 1995), and an extremely α -weak star, BD +80°245 (Fulbright 2000). Carbon rich stars with [C/Fe] > 1 are also excluded. The predicted distributions of stellar fraction, which are shown by the gray scale, are normalized to fit the metallicity distribution of halo stars (Sandage & Fouts 1987). The thick-solid lines indicate the average values of [Eu/Fe] as a function of metallicity, which are calculated from the distributions of stellar fraction. The solid and thin-solid lines indicate, respectively, the

50% and 90% confidence lines, where such stars are expected to appear.

As shown by the predicted stellar distributions in Fig. 2, observational differences between these three cases appear at $[\text{Fe}/\text{H}] \lesssim -3$. In case (c), most of the stars are expected to have enhanced Eu abundance, i.e., $[\text{Eu}/\text{Fe}] > 0$, owing to Eu production solely by massive, short-lived stars. On the other hand, in cases (a) and (b), significant numbers of stars having sub-solar $[\text{Eu}/\text{Fe}]$ are predicted below $[\text{Fe}/\text{H}] \sim -3$ owing to the delayed production of Eu by lower mass stars, as first suggested by Mathews & Cowan (1990). This is outstanding in case (a), due to the largest time delay of Eu production by the lower-mass end of the SN progenitors. We can see that most previous observational data, in many cases only upper limits, distribute between the 90% confidence lines in all cases, which has made it difficult to determine the mass range of the *r*-process site. Our newly obtained data now add detections of Eu, which happen to be the lowest values of $[\text{Eu}/\text{Fe}]$ at $[\text{Fe}/\text{H}] \lesssim -3$. These enable us to distinguish the three cases. The best agreement can be seen in case (a), in which the three stars, together with most other stars from previous observations, are located between the 50% confidence lines at $[\text{Fe}/\text{H}] \lesssim -3$. In case (b), all three stars are located below the average (thick-solid) line, although they remain above the 90% confidence line. In case (c), these stars are located clearly outside the 90% confidence region. We conclude, therefore, that case (a) is most likely to be the *r*-process site, SNe II from low mass progenitors such as $8 - 10M_{\odot}$ stars. The mass of Eu ejected from each $8 - 10M_{\odot}$ star in case (c) is $3.1 \times 10^{-7}M_{\odot}$, which is a reasonable amount from a nucleosynthetic point of view (Wanajo et al. 2002, 2003).

It should be noted that the current study is focused on only the abundance of Eu, as a representative of *r*-process elements. Our abundance analyses for the three extremely metal-poor stars show, however, consistent values of $[\text{Ba}/\text{Eu}]$ with that of the solar *r*-process (Arlandini et al. 1999), when including the estimated errors, as can be seen in Table 3. Hence our result may hold for the heavy *r*-process elements with $Z \geq 56$. The values of $[\text{Sr}/\text{Ba}]$, however, are significantly higher than that of the solar *r*-process. This implies that these three stars exhibit the products of nucleosynthesis of the light *r*-process elements ($Z < 56$) from more massive SNe ($> 10M_{\odot}$). The astrophysical site for this “weak” *r*-processing (Ishimaru & Wanajo 2000) will be discussed in future work.

4. Implications for the *r*-process site

The discussion in § 3 strongly suggests that the production of the *r*-process elements is associated with a small fraction of SNe II near the low-mass end of the range. We can additionally conclude that neutrino winds in the explosions of massive stars face difficulties in being a dominant source of the *r*-process elements. Wanajo et al. (2001) have demonstrated

that an *r*-process in the neutrino winds proceeds from only very massive proto-neutron stars, which might result from massive progenitors such as $20 - 30M_{\odot}$ stars, which is similar to case (b). However, these SNe would generate a significant number of stars with $[\text{Eu}/\text{Fe}] > 0$ at $[\text{Fe}/\text{H}] \lesssim -3$ as can be seen in Figure 2b, which is in conflict with the observed sample. Stars near the high mass-end of the SN progenitors such as hypernovae ($> 20 - 25M_{\odot}$, Maeda & Nomoto 2003) or pair-instability supernovae ($140 - 260M_{\odot}$, Heger & Woosley 2002), similar to case (c), are clearly excluded as the major *r*-process site.

We suggest, therefore, that the dominant source of the *r*-process elements is SN explosions of collapsing O-Ne-Mg cores from $8 - 10M_{\odot}$ stars (Nomoto 1984; Hillebrandt, Nomoto, & Wolff 1984; Wheeler, Cowan, & Hillebrandt 1998). Recently, Wanajo et al. (2003) have demonstrated that the prompt explosion of the collapsing O-Ne-Mg core from a $9M_{\odot}$ star reproduces the solar *r*-process pattern for nuclei with $A > 130$. Their result shows that this type of event is characterized by a lack of α -elements and only a small amount of iron-peak elements, which clearly differs from more massive SNe with iron cores ($> 10M_{\odot}$) that eject both these elements, including low mass SNe ($\sim 11M_{\odot}$) suggested by Sumiyoshi et al. (2001). This is consistent with the fact that the abundances of the heavy *r*-process elements in stars with $[\text{Fe}/\text{H}] \sim -3$ are not related with those of iron-peak elements or of elements with lower atomic numbers as shown by Qian & Wasserburg (2002, 2003).

Tsujimoto, Shigeyama, & Yoshii (2000) determined the major *r*-process site to be stars of $\sim 20M_{\odot}$, based on the relation between the abundances of Mg and Ba as representative of α and *r*-process elements respectively in extremely metal-poor stars. We speculate, however, that α and iron-peak elements in highly *r*-process-enhanced stars such as CS 22892-052 (Sneden et al. 1996) or CS 31082-001 (Hill et al. 2002) do not reflect the chemical compositions of a single $\sim 20M_{\odot}$ star as they suggested but simply that of the ISM at their formation, and only the *r*-process elements come from a single $8 - 10M_{\odot}$ star.

This study clearly shows the importance of detecting low Eu abundances in extremely metal-poor stars to explore the origin of *r*-process elements, which was not possible in previous chemical evolution studies of the *r*-process elements using data from smaller telescopes. Further observation of extremely metal-poor stars in this direction will be needed to confirm our current conclusion.

We thank the Subaru staff for providing such an excellent spectrograph and for assisting with the observations. We also acknowledge the financial support for this research by National Astronomical Observatory of Japan. This work was supported in part by a Grant-in-Aid for Scientific Research (13740129) from the Ministry of Education, Culture, Sports, Science, and Technology of Japan, and by PPARC through grant PPA/O/S/1998/00658.

Table 1. [FE/H] AND RELATIVE ABUNDANCE, [X/FE]

HD 4306			CS 22878-101			CS 22950-046			
	[X/Fe] ^a	n	[X/Fe] ^a	n	σ^b	[X/Fe] ^a	n	σ^b	
Mg I	+0.64	5	0.09	+0.51	5	0.11	+0.30	5	0.16
Ca I	+0.50	10	0.09	+0.26	11	0.10	+0.13	9	0.15
Ti I	+0.42	27	0.09	+0.26	26	0.11	+0.13	15	0.16
Ti II	+0.48	36	0.16	+0.36	37	0.18	+0.16	42	0.20
Fe I	-2.76	168	0.13	-3.14	161	0.14	-3.34	141	0.18
Fe II	-2.79	19	0.13	-3.07	20	0.14	-3.34	17	0.18
Sr II	+0.28	2	0.27	-0.15	2	0.28	-0.18	2	0.30
Ba II	-1.09	2	0.14	-0.73	2	0.16	-1.25	2	0.19
Eu II	-0.57	2	0.16	-0.30	2	0.24	< -0.2	1	...

^a [Fe/H] for Fe I and Fe II.

^b Uncertainty in [Fe/H] or [X/Fe] values.

Table 2. EQUIVALENT WIDTH OF EU LINES

Wavelength Å	Equivalent Width (mÅ)		
	HD 4306	CS 22878-101	CS 22950-046
3819.7	3.8	7.4	<6.8
4129.7	2.2	5.3	
4205.0	2.5:	5.0:	<3.4

Table 3. Abundance ratios among Sr, Ba, and Eu

	HD 4306	CS 22878-101	CS 22950-046	solar [†]
[Sr/Ba]	1.37 ± 0.30	0.58 ± 0.32	1.07 ± 0.36	-0.30
[Ba/Eu]	-0.52 ± 0.21	-0.43 ± 0.29	> -1.05	-0.70

[†]solar system *r*-process abundances by Arlandini et al. (1999)

REFERENCES

Arlandini, C., Käppeler, F., Wissak, K., Gallino, R., Lugaro, M., Busso, M., & Straniero, O., 1999, *ApJ*, 525, 886

Audouze, J. & Silk, J. 1995, *ApJ*, L451, 49

Burris, D. L., Pilachowski, C. A., Armandroff, T. E., Sneden, C., Cowan, J. J., Roe, H. 2000, *ApJ*, 544 302

Carretta, E., Gratton, R., Cohen, J. G., Beers, T. C., Christlieb, N. 2002, *AJ*124, 481

Cohen, J. G., Christlieb, N., Beers, T. C., Gratton, R., Carretta, E. 2002, *AJ*, 124, 470

Depagne, E., Hill, V., Christlieb, N., & Primas, F. 2000, *A&A*, 364, 6

Fields, B. D., Truran, J. W., & Cowan, J. J. 2002, *ApJ*, 575, 845

Freiburghaus, C., Rosswog, S., & Thielemann, F. -K. 1999, *ApJ*, 525, L121

François, P., et al. 2003, *A&A*, 403, 1105

Fulbright, J. P. 2000, *AJ*, 120, 1841

Gilroy, K. K., Sneden, C., Pilachowski, C. A., & Cowan, J. J. 1988, *ApJ*, 327, 298

Gratton, R. G., Sneden, C. 1994, *A&A*, 287, 927

Heger, A. & Woosley, S. E. 2002, *ApJ*, 567, 532

Hill, V., et al. 2002, *A&A*, 387, 560

Hillebrandt, W., Nomoto, K., & Wolff, R. G. 1984, *A&A*, 133, 175

Houdashelt, M.L., Bell, R.A., & Sweigart, A.V. 2000, *ApJ*, 119, 1448

Ishimaru, Y., Wanajo, S. 1999, *ApJ*, L511, 33

Ishimaru, Y. & Wanajo, S. 2000, in *First Stars*, ed. A. Weiss, T. Abel, & V. Hill (Berlin: Springer), 189

Ishimaru, Y., Prantzos, N., & Wanajo, S. 2003, *Nucl. Phys. A*, in press

Johnson, J. A. 2002, *ApJS*, 139, 219

Johnson, J. A. & Bolte, M. 2002, *ApJ*, 579, 616

Kurucz, R. L., 1993, CD-ROM 13, ATLAS9 Stellar Atmospheres Programs and 2km/s Grid (Cambridge: Smithsonian Astrophys. Obs.)

Kurucz, R. L., 1995, CD-ROM 23, (Cambridge: Smithsonian Astrophys. Obs.)

Lawler, J. E., Wickliffe, M. E., Den Hartog, E. A. & Sneden, C. 2001, ApJ, 563, 1075

Maeda, K. & Nomoto, K. 2003, ApJ, submitted (astro-ph/0304172)

Mathews, G. J., Cowan, J. J. 1990, Nature, 345, 491

McWilliam, A., Preston, G. W., Sneden, C., & Searle, L. 1995, AJ, 109, 2757

McWilliam, A. 1998, AJ, 115, 1640

Noguchi, K., et al. 2002, PASJ, 54, 855

Nomoto, K. 1984, ApJ, 277, 791

Nomoto, K., Hashimoto, M., Tsujimoto, T., Thielemann, F. -K., Kishimoto, N., Kubo, Y., & Nakasato, N. 1997a, Nucl. Phys. A, 616, 79

Nomoto, K., et al. 1997b, Nucl. Phys. A, 621, 467

Norris, J.E., Bessell, M.S., & Pickles, A.J. 1988, ApJS, 58, 463

Norris, J. E., Ryan, S. G., & Beers, T. C. 2001, ApJ, 561, 1034

Qian, Y. -Z. & Wasserburg, G. J. 2002, ApJ, 567, 515

Qian, Y. -Z. & Wasserburg, G. J. 2003, ApJ, 588, 1099

Ryan, S. G., Norris, J. E., & Bessell, M. S. 1991, AJ, 102, 303

Ryan, S. G., Norris, J. E., & Beers, T. C. 1996, ApJ, 471, 254

Sandage, A. & Fouts, G. 1987, AJ, 97, 74

Shetrone, M. D. 1996, AJ, 112, 1517

Skrutskie, M.F., et al. 1997, in The Impact of Large Scale Near-IR Sky Surveys, ed. F. Garzon et al. (Dordrecht: Kluwer), p. 187

Sneden, C., McWilliam, A., Preston, G. W., Cowan, J. J., Burris, D. L., & Armosky, B. J. 1996, ApJ, 467, 819

Sumiyoshi, K., Terasawa, M., Mathews, G. J., Kajino, T., Yamada, S., & Suzuki, H. 2001, *ApJ*, 562, 880

Travaglio, C., Galli, D., Gallino, R., Busso, M., Ferrini, F., Straniero, O. 1999, *ApJ*, 521, 691

Tsujimoto, T., Shigeyama, T., & Yoshii, Y. 2000, *ApJ*, L531, 33

Wanajo, S., Kajino, T., Mathews, G. J., & Otsuki, K. 2001, *ApJ*, 554, 578

Wanajo, S., Itoh, N., Ishimaru, I., Nozawa, S. & Beers, T. C. 2002, *ApJ*, 577, 853

Wanajo, S., Tamamura, M., Itoh, N., Nomoto, K., Ishimaru, I., Beers, T. C., & Nozawa, S. 2003, *ApJ* preprint doi:10.1086/376617

Westin, J., Sneden, C., Gustafsson, B., Edvardsson, B., Cowan, J. J. 1998, *BAAS*, 30, 1317

Wheeler, J. C., Cowan, J. J., & Hillebrandt, W. 1998, *ApJ*, L493, 101

Woolf, V. M., Tomkin, J., & Lambert, D. L. 1995, *ApJ*, 453, 660

Woosley, S. E., Wilson, J. R., Mathews, G. J., Hoffman, R. D., & Meyer, B. S. 1994, *ApJ*, 433, 229

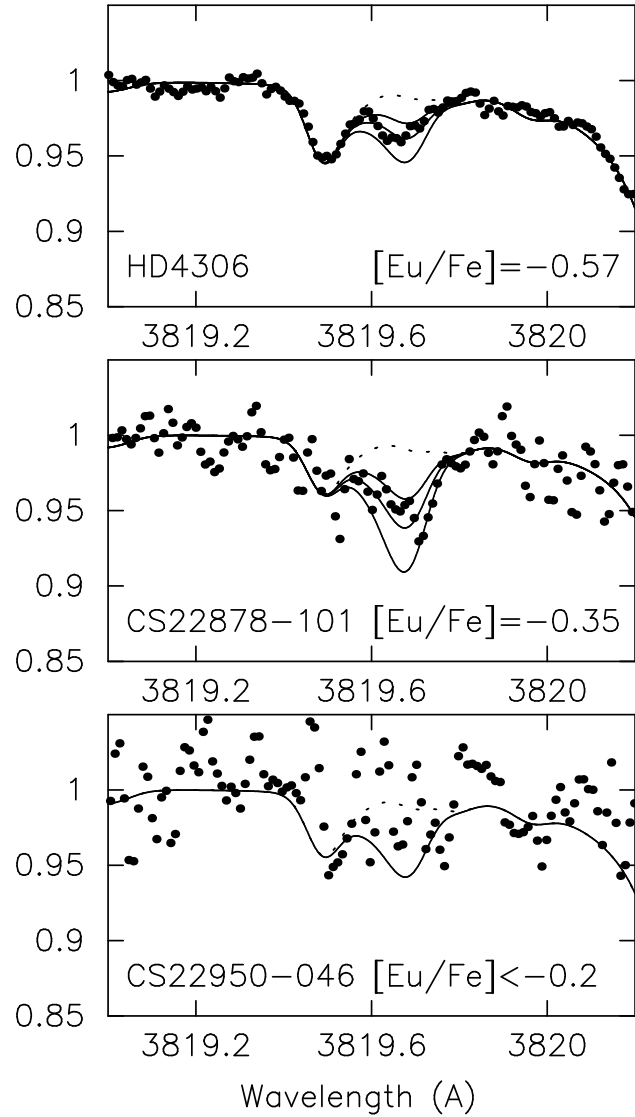


Fig. 1.— Comparison of the observed spectra (dots) and synthetic ones (lines) near the Eu II 3819.7 Å line. For HD 4306 and CS 22878–101, three synthetic spectra differ in step of $\Delta[\text{Eu}/\text{Fe}] = 0.2$ dex are shown by solid lines. Central line is calculated for the Eu abundance presented in each panel. The solid line in the panel for CS 22950–046 indicates the synthetic spectrum for the upper limit of Eu abundance presented in the panel (see text). Dotted lines are the spectra calculated assuming no Eu contribution.

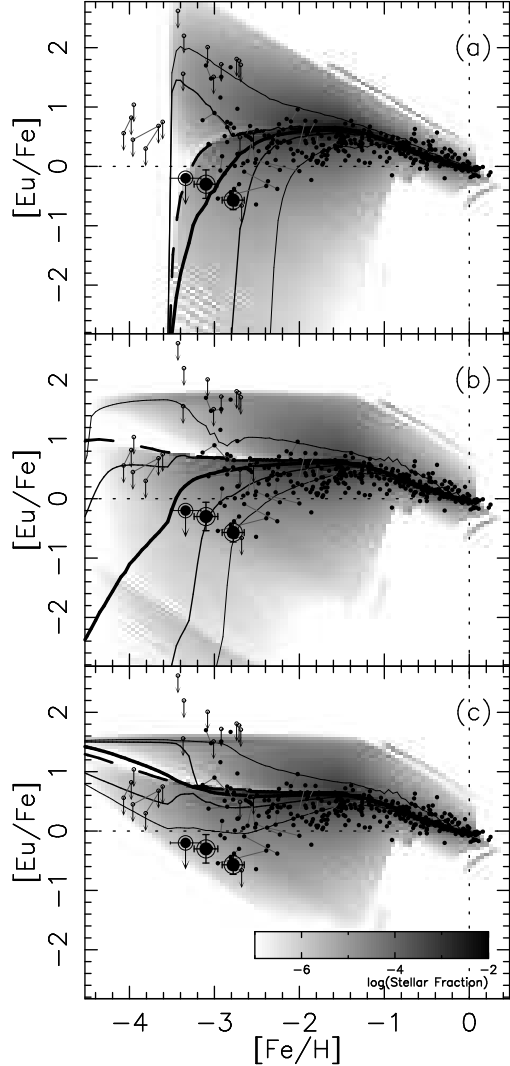


Fig. 2.— Comparison of the observed data and model predictions of the $[\text{Eu}/\text{Fe}]$ vs. $[\text{Fe}/\text{H}]$ relation. The r -process site is assumed to be SNe II of (a) $8 - 10 M_{\odot}$, (b) $20 - 25 M_{\odot}$, and (c) $> 30 M_{\odot}$ stars. The predicted distributions of stellar fraction are given in the gray scale. The thick-solid lines indicate the averages of stellar abundance distributions as a function of $[\text{Fe}/\text{H}]$, and the 50% and 90% confidence intervals are shown by solid and thin-solid lines, respectively. The average abundance of the ISM given from a one-zone chemical evolution model are also denoted by the thick-dashed lines. Other observational data (small circles) are taken from Gratton & Sneden (1994); McWilliam et al. (1995); McWilliam (1998); Woolf, Tomkin, & Lambert (1995); Ryan, Norris, & Beers (1996); Shetrone (1996); Sneden et al. (1996); Westin et al. (1998); Depagne et al. (2000); Burris et al. (2000); Fulbright (2000); Norris, Ryan, & Beers (2001); Carretta et al. (2002); Johnson (2002); Johnson & Bolte (2002); François et al. (2003); Honda (private communication).